THE JOURNAL OF BIOLOGICAL CHEMISTRY

Vol. 274, No. 38, Issue of September 17, pp. 26838–26842, 1999
Printed in U.S.A.

Salt Links Dominate Affinity of Antibody HyHEL-5 for Lysozyme through Enthalpic Contributions*

(Received for publication, May 13, 1999)

Jamie A. Wibbenmeyer‡, Peter Schuck§, Sandra J. Smith-Gill¶, and Richard C. Willson‡‖****

From the ‡Department of Biology and Biochemistry, University of Houston, Houston, Texas 77024-4792, the §Molecular Interactions Resource, Bioengineering and Physical Science Program, National Institutes of Health, Bethesda, Maryland 20892, the ¶NCI, National Institutes of Health, Frederick Cancer Research and Development Center, Frederick, Maryland 21702-1201, and the ‖Department of Chemical Engineering, University of Houston, Houston, Texas 77024-4792

The binding of murine monoclonal antibody HyHEL-5 to lysozyme has been the subject of extensive crystallographic, computational, and experimental investigations. The complex of HyHEL-5 with hen egg lysozyme (HEL) features salt bridges between Fab heavy chain residue Glu^{50}, and Arg^{45} and Arg^{68} of HEL. This interaction has been predicted to play a dominant role in the association on the basis of molecular electrostatics calculations. The association of aspartic acid and glutamine mutants at position 50_H of the cloned HyHEL-5 Fab with HEL and bobwhite quail lysozyme (BQL), an avian variant bearing an $Arg^{68} \rightarrow$ Lys substitution in the epitope, was characterized by isothermal titration calorimetry and sedimentation equilibrium. Affinities for HEL were reduced by 400-fold ($E50_HD$) and 40,000-fold ($E50_HQ$) ($\Delta\Delta G°$ estimated at 4.0 and 6.4 kcal mol^{-1}, respectively). The same mutations reduce affinity for BQL by only 7- and 55-fold, respectively, indicating a reduced specificity for HEL. The loss of affinity upon mutation is in each case primarily due to an unfavorable change in the enthalpy of the interaction; the entropic contribution is virtually unchanged. An enthalpy-entropy compensation exists for each interaction; $\Delta H°$ decreases, while $\Delta S°$ increases with temperature. The ΔCp for each mutant interaction is less negative than the wild-type. Mutant-cycle analysis suggests the mutations present in the HyHEL-5 Fab mutants are linked to those present in the BQL with coupling energies between 3 and 4 kcal mol^{-1}.

The interaction of the murine IgG_1 κ antibody HyHEL-5[1] with lysozyme has been used as a model system in the investigation of protein-protein interactions (1–5). The epitope was first mapped using avian species variant lysozymes (4) and was later verified by three-dimensional crystal structures of Fab-lysozyme complexes (1, 6–8). The interaction of HyHEL-5 with a variety of lysozymes has been characterized thermodynamically (9, 10) and kinetically (11). The prominent structural feature of the HyHEL-5/hen egg lysozyme (HEL[1]) interaction is the presence of salt bridges formed in the interface between glutamate residue 50 in the heavy chain of the antibody ($E50_H$) and arginine residues 45 and 68 of the lysozyme (1, 7, 8). These bonds are found buried in the interface, far removed from solvent, in an environment of low dielectric constant. The high affinity of the interaction has been attributed to the presence of these salt links, and computational analyses of the interaction have focused on these electrostatic interactions (12–15).

We have recently cloned the genes for the Fab fragment of HyHEL-5 into *Escherichia coli* and expressed and refolded an active Fab, whose interactions with HEL and bobwhite quail lysozyme (BQL) are energetically similar to those of the whole IgG (16). Site-directed mutants of the Fab at $E50_H$ were prepared to address the role of the salt links in the interaction with antigen. The interaction of each mutant with HEL and BQL, an avian variant containing an arginine to lysine mutation at position 68, was characterized using isothermal titration calorimetry (ITC) and/or sedimentation equilibrium.

In this paper, we report on the energetic contributions of the salt links formed between residue $E50_H$ in the Fab and arginine residues 45 and 68 in lysozyme. By mutating a single amino acid residue, the affinity and specificity of the interaction has been dramatically reduced. Furthermore, our results demonstrate the dominantly enthalpic character of bonds formed between charged residues in this highly desolvated interface.

EXPERIMENTAL PROCEDURES

Site-directed Mutagenesis of Recombinant HyHEL-5 Fab—Mutagenesis was done using crossover polymerase chain reaction or the M13 method as described by Kunkel *et al.* (17). Polymerase chain reaction was performed in a Perkin-Elmer Gene Amp System 2400 with *Taq* DNA polymerase from Promega. Three polymerase chain reaction reactions were necessary for the $E50_HQ$ mutant. Two primers (GCTACCACTCCCGGGTAAAAT**CTG**TCCAATCCA (sense) and TGGATTGGA**CAG**ATTTTACCCGGGAGTGGTAGC (antisense); both from Bioserve Biotechnologies) were designed to introduce both the mutant nucleotide sequence (shown in bold) and an additional 1-base pair change to introduce a *Sma*I site (shown underlined). The first set of reactions contained the heavy chain DNA template (pET MH5wt), the sense primer containing the mutation, and a T7 reverse primer (T7 AS), while the companion reaction used the antisense primer containing the complementary sequence along with a T7 forward primer (T7 S). After the polymerase chain reaction was completed (15 cycles of 94 °C/55 °C/74 °C for 1 min each with a final 6-min extension at 72 °C), an aliquot of each purified fragment was added to a final reaction containing only the T7 sense and antisense primers. This "crossover" reaction resulted in a 900-base pair band which was double-digested with *Bam*HI and *Hin*dIII to release a 480-base pair fragment to subclone into the double-digested (*Bam*HI/*Hin*dIII) and dephosphorylated pET MH5wt vector. Positive clones bearing the primer-encoded *Sma*I site were identified by the appearance of a band at 1200 base pairs when restricted by *Sma*I (the vector contains one constitutive *Sma*I restriction site) and further verified by DNA sequencing on an automated ABI fluorescence se-

* This work was supported by a Welch Foundation grant (to R. C. W.). The costs of publication of this article were defrayed in part by the payment of page charges. This article must therefore be hereby marked "*advertisement*" in accordance with 18 U.S.C. Section 1734 solely to indicate this fact.

** To whom correspondence should be addressed. Tel.: 713-743-4308; Fax: 713-743-4323; E-mail: willson@uh.edu.

[1] The abbreviations used are: HEL, hen egg lysozyme; BQL, bobwhite quail lysozyme; ITC, isothermal titration calorimetry; Fab, antigen-binding fragment of the immunoglobulin; wt, wild-type HyHEL-5 Fab; $E50_HD$, HyHEL-5 Fab mutant in which Glu at position 50 in the variable region of the heavy chain is substituted with Asp; $E50_HQ$, HyHEL-5 Fab mutant in which Glu at position 50 in the variable region of the heavy chain is substituted with Gln.

quencer (University of Texas Health Science Center-Houston) prior to protein expression.

The $E50_HD$ mutant was prepared by the Kunkel method after subcloning a *Bam*HI/*Hin*dIII fragment of the heavy chain gene into M13mp19. The primer used, GGA**GAT**ATCTTACCTGGAAGTGGT, included a silent mutation to insert an *Eco*RV site, and positive clones were identified by the appearance of a 1.6-kilobase band upon digestion with *Eco*RV. The mutated fragment was subcloned into the MH5wt vector and the sequence verified by DNA sequencing.

Purification of Mutant Proteins—The mutant proteins were purified as described previously for the wild-type Fab (16). Briefly, 2-liter cultures of induced cells expressing either the mutant heavy chain or the wild-type light chain were harvested by centrifugation. Cells containing the light chain were lysed by French Press. Inclusion bodies were washed once with buffer (100 mM Tris, 2.5 mM EDTA, 0.02% Tween 20, pH 7.9), recentrifuged, and the final pellet resuspended in denaturation buffer (100 mM Tris, 6 M guanidine HCl, 2.5 mM EDTA, 0.4 M L-arginine HCl, pH 7.9) to a final protein concentration of 2 mg/ml. Whole cells expressing the heavy chain were dissolved in the denaturation buffer (plus 100 mM dithiothreitol) to a protein concentration of 2 mg/ml. After stirring at room temperature for 1 h, the solutions were mixed in a 1:2 (light:heavy) molar ratio in the presence of 4 mM glutathione and diluted 10-fold with denaturation buffer. The solutions were exhaustively dialyzed against Tris buffer to remove, through successive changes, the guanidine and L-arginine.

The refolded protein was concentrated using tangential flow filtration and purified by Q Sepharose and nickel-charged chelating Sepharose Fast Flow chromatography. The resulting protein was at least 95% pure based on SDS-polyacrylamide gel electrophoresis and sedimentation equilibrium experiments.

Isothermal Titration Calorimetry—Hen egg lysozyme (2 times crystallized) was purchased from Worthington Biologicals. BQL was prepared from eggs purchased from Stevenson's Game Bird Farm (Riverside, TX) as described by Shick *et al*. (9). Concentrations of all proteins were determined spectrophotometrically using extinction coefficients reported previously (16, 18).

ITC was performed in an MCS Isothermal Titration Calorimeter (Microcal) essentially as in previous work (11). Briefly, the calorimeter was equilibrated overnight at a temperature 5 °C below that intended for the experiment. HyHEL-5 Fab and HEL or BQL were allowed to co-dialyze overnight in 100 mM sodium phosphate buffer containing 150 mM NaCl (ITC buffer), pH 8.0. Experiments were also performed in Tris buffer to measure protonation effects. A typical experiment used 1.7 ml of HyHEL-5 Fab (about 20 μM) in the sample cell. The antigen (HEL or BQL, about 300 μM) was titrated into the HyHEL-5 Fab in 16 injections of 10 μl, 300 s apart. An initial injection of 2 μl was made to clear the syringe of any Fab from the sample cell which might have mixed with the lysozyme in the syringe during equilibration. All titrations were performed at least in duplicate. The reported errors are the standard deviations.

Data analysis was performed using the software program Origin, and is based on the amount of heat liberated upon association as described (19). The change in Gibbs free energy upon association, $\Delta G°$, was calculated using the formula,

$$\Delta G° = -RT\ln K_a \qquad \text{(Eq. 1)}$$

where R is the gas constant and T is the absolute temperature. The entropy change of association, $\Delta S°$, was calculated using,

$$\Delta G° = \Delta H° - T\Delta S° \qquad \text{(Eq. 2)}$$

where $\Delta H°$ is the measured enthalpy of association of the reaction at temperature T.

The equivalence number, n, K_a, and $\Delta H°$ could be determined for all interactions except the $E50_HQ$/BQL and the $E50_HA$ associations, which were too weak to be measured by ITC.

Sedimentation Equilibrium Experiments—Sedimentation equilibrium experiments were performed in a Beckman Optima XL-A analytical ultracentrifuge using an 8-hole An 50 Ti rotor, at several rotor speeds between 15,000 and 25,000 rpm at 17 °C. Two-channel epon centerpieces were filled with an 0.18-ml sample, giving column heights of approximately 5 mm; the compartment adjoining each sample was filled with ITC buffer. Loading concentrations of Fab and lysozyme were varied in a series of experiments, covering a range of concentrations from 0.1 to 44 μM Fab and 2 to 30 μM lysozyme. The buoyant molar mass of lysozyme $M^*_{Lys} = M_{lys}(1 - \bar{\nu}\rho)$ and of the Fab fragments $m^*_{Fab} = M_{fab}(1 - \bar{\nu}\rho)$ were measured in independent sets of experiments. The absence of non-ideality effects or self-aggregation in the measured sedimentation profiles of the individual species at high concentrations was demonstrated by their constant apparent molar mass in the centrifugal field over the entire range of concentrations used in the experiments. Sedimentation equilibrium was established by random radial distribution of the difference of signals from successive scans.

The absorbance distributions were measured at wavelengths of 250, 280, or 305 nm, chosen so that the measured maximum absorbance was smaller than 1.5 OD. The extinction coefficients were based on a molar extinction coefficient of 83,800 $OD_{280\ nm}\ M^{-1}\ cm^{-1}$ for the Fab fragments and 37,700 $OD_{280\ nm}\ M^{-1}\ cm^{-1}$ for the lysozyme. The extinction coefficients at 230, 250, and 305 nm were measured in the analytical ultracentrifuge in sedimentation equilibrium experiments with the single species, by taking multiple scans at the respective wavelengths and obtaining the ratio of the absorbance at the reference radius after modeling the radial absorbance distribution (see below).

Data analysis employed the global least-squares modeling of between 5 and 13 absorbance profiles $\alpha_\lambda(r)$ taken at different loading concentrations, rotor speeds, and wavelengths. The fitting function for the mixtures was the sum of the expressions for the distributions of individual components in the centrifugal field,

$$\alpha_\lambda(r) = \alpha_{\lambda,Lys}(r_0)\exp\left[M^*_{Lys}\frac{\omega^2}{2RT}(r^2 - r_0^2)\right] + \alpha_{\lambda,Fab}(r_0)\exp\left[M^*_{Fab}\frac{\omega^2}{2RT}(r^2 - r_0^2)\right] + \alpha_{\lambda,Fab}(r_0)\alpha_{\lambda,Lys}(r_0)\epsilon_\lambda d\,\exp\left[\ln K_a + (M^*_{Fab} + M^*_{Lys})\frac{\omega^2}{2RT}(r^2 - r_0^2)\right] + \delta \qquad \text{(Eq. 3)}$$

where $\alpha_{\lambda,Lys}(r)$ and $\alpha_{\lambda,Fab}(r_0)$ denote the absorbance contribution of free Fab fragment or lysozyme, respectively, at a reference radius r_0, ω denotes the angular velocity of the rotor, R denotes the gas constant, T denotes the absolute temperature, δ denotes a baseline offset, K_a denotes the association equilibrium constant in molar units, d denotes the optical path length, and ϵ_λ denotes a predetermined extinction coefficient,

$$\epsilon_\lambda = \frac{\epsilon_{\lambda,Fab} \times \epsilon_{\lambda,Lys}}{\epsilon_{\lambda,Fab} + \epsilon_{\lambda,Lys}} \qquad \text{(Eq. 4)}$$

which transforms the association constant from absorbance units into molar units. Fitting parameters local to each of the data sets were $\alpha_{\lambda,Lys}(r_0)$, $\beta_{\lambda,Fab}(r_0)$, and δ; the global fitting parameter was $ln(K_a)$ (20). Global fits were performed using the modeling software MLAB (Civilized Software, Inc., Bethesda, MD). Confidence intervals were estimated using projections of the objective function (21) and F-statistics (22), taking into account propagated errors resulting from the uncertainty in the determination of the buoyant molar masses of the lysozyme (1.6%) and the Fab fragments (4.2%).

RESULTS

Throughout the denaturation and refolding process, each of the mutant proteins behaved identically to the wild-type HyHEL-5 Fab, eluting at the same gradient positions from the Q Sepharose and the metal-chelate columns. Sedimentation equilibrium experiments demonstrated that each of the recombinant proteins was non self-aggregating, all running with the same apparent molar mass at concentrations up to 40 μM. Preliminary x-ray crystallographic analysis indicates the $E50_HQ$/HEL crystals are isomorphous with the proteolytic HyHEL-5 Fab·HEL complex (PDB 3HFL; 1).[2]

Isothermal Titration Calorimetry—A typical isothermal titration calorimetry experiment is illustrated in Fig. 1. Table I lists the values determined at temperatures ranging from 10 to 30 °C in ITC buffer. To correct for any heat of dilution, the integrated areas of the last three injections (after saturation) were averaged and subtracted from the raw data. Heats of dilution were less than 1 kcal mol^{-1} at Fab concentrations around 20 μM. Experimental equivalence ratios, N, are also shown.

The affinity of the wild-type Fab/HEL interaction has been estimated to be about $4 \times 10^{10}\ M^{-1}$ at 25 °C (23). The HEL

[2] M. D. Miller, personal communication.

affinity at 25 °C of the $E50_HQ$ mutant was reduced by 40,000-fold, while that of the $E50_HD$ was reduced by 400-fold, corresponding to an overall decrease in free energy of 6.4 and 4.0 kcal mol^{-1}, respectively. An $E50_HA$ mutant showed no evidence of HEL binding in ITC experiments, indicating a decrease of at least 10^5-fold in affinity for the single mutation based on a lower ITC detection limit of 1×10^5 M^{-1}.

The affinity of wild-type Fab association with BQL, the R68K avian mutant, has been measured by ITC to be 6.6×10^6 M^{-1} at 25 °C (16). Only the $E50_HD$ mutant showed BQL affinity high enough to be measured through ITC; the K_a of the interaction was 1.0×10^6 M^{-1}, a 6.6-fold decrease in the affinity, accounting for a $\Delta\Delta G°$ of 1.1 kcal mol^{-1}.

The K_a of each mutant/lysozyme interaction studied is lower than that of the wild-type Fab/HEL, and decreases as the temperature increases. Both $\Delta H°$ and $\Delta S°$ become more negative throughout the temperature range, leading to a relatively constant $\Delta G°$ (Fig. 2). The ΔCp of each interaction is less negative than that of the wild-type Fab/lysozyme interactions (Table II). Negligible protonation effects ($\leq$0.1 mol mol^{-1}) were observed for all associations.

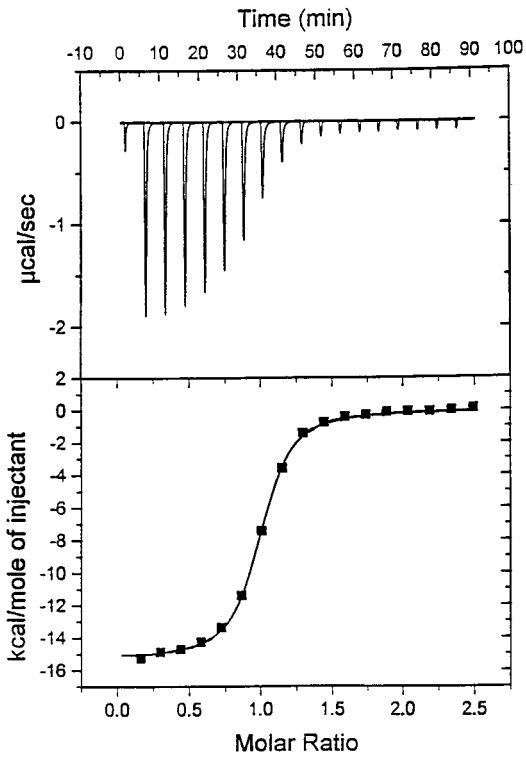

FIG. 1. **Typical results for isothermal titration calorimetry of the interaction between HyHEL-5 Fab mutants and HEL or BQL.** Titration of the HyHEL-5 Fab mutant $E50_HD$ (20 μM) with HEL (250 μM) at 25 °C.

Sedimentation Equilibrium—Sedimentation equilibrium experiments resulted in a K_a of 1.16×10^5 M^{-1} (error limits 1.3×10^4 to 1.6×10^5) for the $E50_HQ$/BQL interaction at 17 °C, a 55-fold decrease in the affinity, corresponding to a $\Delta\Delta G°$ of 2.7 kcal mol^{-1} from the wild-type interaction.

Double-mutant Cycle Analysis—To further understand the energetic changes observed upon mutating position 50_H in the HyHEL-5 Fab, double-mutant cycles were constructed (Fig. 3). Each cycle was based on the substitution at position 50_H of the Fab, and the R68K substitution (and other mutations known to exert much smaller effects) in BQL.

In each of the interactions examined, the sums of $\Delta\Delta G°$ of the single-mutant interactions were different from those obtained for the double-mutant interactions, indicating coupling between the mutations (Table III). Subtracting the sum of the free energy changes of the two single mutations from that of the double-mutant gave a coupling energy of +2.9 kcal mol^{-1} for the wt/HEL → $E50_HD$/BQL pathway and +3.7 kcal mol^{-1} for the wt/HEL → $E50_HQ$/BQL pathway (Fig. 3).

DISCUSSION

Mutational Effects on the Affinity of the Interaction—In the HyHEL-5/lysozyme interaction, glutamic acid residues at heavy chain positions 50 in CDR 1 and 35 in CDR 2, have long been predicted to form the core of the functional combining site. In crystal structures, $E50_H$ is juxtaposed with and believed to form salt links to arginines at positions 45 and 68 in the HEL molecule. In BQL, which bears an arginine to lysine mutation at position 68, a new water molecule appears in the interface at the position formerly occupied by the terminal nitrogens of Arg^{68}. These residues are buried in the center of the interface, far removed from solvent, in an environment of low dielectric constant. To study the role of the glutamate at position 50 in these interactions, three mutations, an alanine, aspartate, and glutamine, were introduced into the Fab and the association with HEL and BQL measured by either ITC or sedimentation equilibrium. Substitution of Ala, which both neutralizes the charge and decreases the length of the side chain, produced the greatest affinity changes. When the charge was maintained but the length of the side chain decreased, in the $E50_HD$ mutant, binding was decreased by 400-fold (HEL) and 6.6-fold (BQL). The $E50_HQ$ maintained the side chain length, but neutralized the charge of the side chain decreasing the binding by 40,000-

TABLE I
Titration calorimetric energetics of interaction between HyHEL-5 Fab mutants and HEL or BQL

Temperature	$\Delta H°$	K_a ($\times 10^{-5}$)	$\Delta G°$	$\Delta S°$	Equivalence ratio
°C	*kcal mol^{-1}*	*M^{-1}*	*kcal mol^{-1}*	*cal mol^{-1} K^{-1}*	
$E50_HD$/HEL association					
9.9	−12.6 ± 0.10	1460 ± 298	−10.6 ± 0.11	−7.36 ± 0.13	0.87 ± 0.01
16.6	−15.4 ± 0.04	979 ± 242	−10.6 ± 0.11	−16.5 ± 0.23	0.85 ± 0.00
25.0	−18.7 ± 0.56	562 ± 168	−10.5 ± 0.13	−27.2 ± 1.44	0.88 ± 0.00
30.1	−20.3 ± 0.10	447 ± 156	−10.6 ± 0.16	−31.9 ± 0.27	0.90 ± 0.00
$E50_HQ$/HEL association					
11.0	−12.5 ± 0.34	17.0 ± 3.0	−8.07 ± 0.11	−15.7 ± 0.80	0.93 ± 0.04
18.1	−13.5 ± 0.35	10.3 ± 6.7	−8.01 ± 0.02	−18.8 ± 1.14	0.90 ± 0.03
25.1	−16.4 ± 0.44	9.4 ± 4.3	−8.09 ± 0.27	−27.8 ± 0.55	0.89 ± 0.00
30.2	−17.2 ± 0.43	4.4 ± 0.3	−7.83 ± 0.04	−31.0 ± 1.26	0.88 ± 0.05
$E50_HD$/BQL association					
10.4	−15.3 ± 0.01	35.8 ± 5.0	−8.50 ± 0.01	−23.9 ± 0.01	0.95 ± 0.01
16.6	−16.9 ± 0.29	22.1 ± 2.0	−8.37 ± 0.07	−29.4 ± 0.76	0.85 ± 0.03
25.1	−17.9 ± 0.42	9.7 ± 8.0	−8.22 ± 0.06	−32.2 ± 1.29	0.88 ± 0.03
30.1	−18.1 ± 1.08	7.4 ± 1.0	−8.17 ± 0.04	−30.1 ± 0.25	0.86 ± 0.00

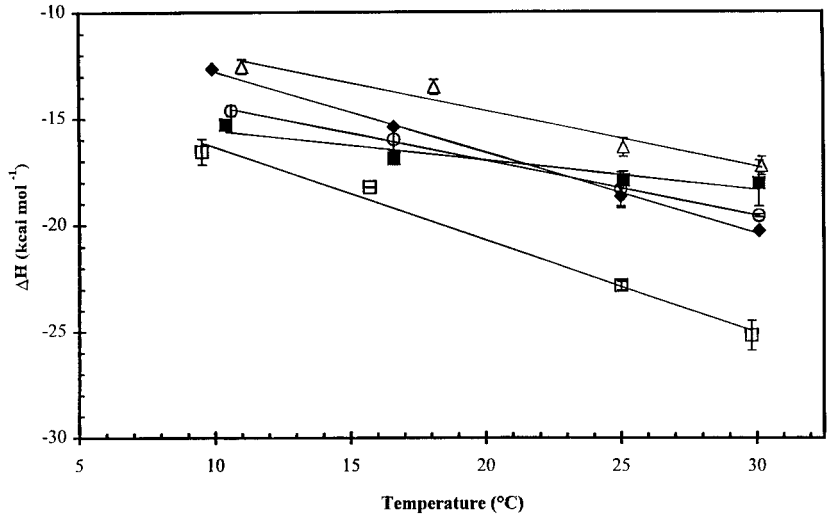

FIG. 2. **Temperature dependence of enthalpies of association of interactions between HyHEL-5 Fab mutants and HEL and BQL.** Wt Fab/HEL (□) and wt Fab/BQL (○) results from Wibbenmeyer *et al.* (16); $E50_HD$/HEL (♦); $E50_HQ$/HEL (△); $E50_HD$/BQL (■).

TABLE II
Energetic contributions to association of Fab mutants with HEL or BQL
Values were obtained from ITC at 25 °C or sedimentation equilibrium at 17 °C as described under "Experimental Procedures."

Lysozyme	Fab	K_a	$\Delta H°$	$\Delta G°$	$T\Delta S°$	ΔCp	$\Delta\Delta G°$	$\Delta\Delta H°$	$\Delta T\Delta S°$	$\Delta\Delta Cp$
		M^{-1}	*kcal mol*$^{-1}$	*kcal mol*$^{-1}$	*kcal mol*$^{-1}$	*cal mol*$^{-1}$ *K*$^{-1}$	*kcal mol*$^{-1}$	*kcal mol*$^{-1}$	*kcal mol*$^{-1}$	*cal mol*$^{-1}$ *K*$^{-1}$
	Wt Fab	4×10^{10} [a]	−22.8 ± 0.2	−14.50	−8.3	−410 ± 18	0	0	0	0
HEL	$E50_HD$	5.6×10^7	−18.7 ± 0.6	−10.5 ± 0.1	−8.2 ± 0.4	−264 ± 39	4.0	4.2	0.1	146
	$E50_HQ$	9.4×10^5	−16.4 ± 0.4	−8.1 ± 0.3	−8.3 ± 0.2	−385 ± 11	6.4	6.5	0.0	25
	Wt Fab	6.6×10^6 [b]	−18.3 ± 0.8	−9.3 ± 0.1	−9.0 ± 0.7	−258 ± 8	0	0	0	0
BQL	$E50_HD$	1.0×10^6	−18.1 ± 1.1	−8.2 ± 0.0	−9.9 ± 1.0	−139 ± 30	1.1	0.2	0.9	119
	$E50_HQ$	1.2×10^5	Sedimentation	−6.7; +0.2/−1.2	Sedimentation	Sedimentation	2.7			

[a] From Lavoie *et al.* (23).
[b] From Wibbenmeyer *et al.* (16).

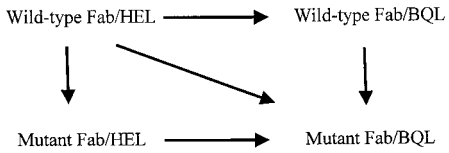

FIG. 3. **Double-mutant cycle to test for coupling between HyHEL-5 Fab 50_H mutations and the BQL R68K mutation.**

TABLE III
Calculation of coupling energy from double-mutant cycle

Interaction	$E50_HD$	$E50_HQ$
wt Fab/HEL → wt Fab/BQL	5.2	5.2
wt Fab/HEL → mutant Fab/HEL	4.0	6.4
Total $\Delta\Delta G°_{association}$ (kcal mol^{-1})	9.2	11.6
wt Fab/HEL → mutant Fab/BQL	6.3	7.9
Coupling energy (kcal mol^{-1})	2.9	3.7

fold (HEL) and 55-fold (BQL), reducing the free energy of association by more than 6 kcal mol^{-1} in the HEL interaction and 2.7 kcal mol^{-1} in the BQL interaction.

Mutational studies of interacting surfaces in other proteins have demonstrated that only a small number of residues play a dominant role in binding (24). For example, in the interaction of human growth hormone with its receptor, 11 residues constitute the functional hormone epitope; mutation of either of two tryptophans to alanine, reduces association energy by over 4.5 kcal mol^{-1}.

The mutational $\Delta\Delta G°$ of 6.4 kcal mol^{-1} for $E50_HQ$/HEL and 4.0 kcal mol^{-1} for $E50_HD$/HEL are generally consistent with those predicted by Slagle *et al.* (14) who calculated a $\Delta\Delta G_{electrostatic}$ of +11 kcal mol^{-1} for $E50_HQ$ and +2.5 kcal mol^{-1} for $E50_HD$. Most importantly, in both the model and the experimental results, each mutation yields a positive $\Delta\Delta G°$ and the effect of the $E50_HQ$ mutation is larger.

Thermodynamic Characterization of the Interactions—For both mutants studied, the entropic contribution to HEL association was indistinguishable from that of the wild-type Fab (−8.3 kcal mol^{-1}) at 25 °C (Table II). $\Delta H°$, in contrast, decreased by an average of 5.3 kcal mol^{-1} and by up to 6.5 kcal mol^{-1} from that of the wild-type Fab. Consequently, the affinity decrease for each mutant results almost entirely from loss of favorable enthalpic interactions.

For each mutant studied, the loss of enthalpic contribution to HEL association is among the highest reported, which may be due to the favorable desolvated local environment in which the electrostatic interaction occurs. Ross and Subramanian (27) have suggested that salt links may contribute to enthalpy changes when formed in an environment of low dielectric constant. Other studies have associated salt bridge formation in desolvated environment with enthalpic contributions (9, 24). Entropic contributions appear to play a greater role when electrostatic bonds are formed in solvated environments, where their contributions to binding affinity are lower (*e.g.* the anti-lysozyme antibody HyHEL-10) (27).

In each of the mutant Fab/lysozyme interactions examined, enthalpy-entropy compensation exists (Table I). As the temperature increases, the enthalpy change of each interaction becomes more favorable (Fig. 2), while the entropy change becomes less favorable and affinity is relatively constant. This behavior (and the observed negative values of ΔCp) has been suggested to be an indicator of hydrophobic interactions. The unfavorable entropy change upon association may arise from loss of protein translational, rotational, and conformational degrees of freedom on complex formation, part of which arises

from the stabilization of the mobile loop found in the HyHEL-5 epitope. Crystal structures reveal that, upon complex formation, this epitope is immobilized (1). Amide exchange studies show that residues in HEL far removed from the interface are also perturbed upon binding, possibly altering the dynamics of the molecule and adding to an unfavorable entropy (29). The ordering of water molecules in and around the interface will decrease entropy, while likely contributing positively to the enthalpy, while burial of hydrophobic residues will increase the solvent entropy through water liberation.

The ΔCp value calculated for each mutant complex was less negative than that obtained for the wild-type HyHEL-5 Fab (Table II). For the $E50_HD$/BQL interaction, ΔCp is only approximately one-half of that of the wild-type Fab/BQL interaction.

A negative ΔCp has been interpreted as an indication of hydrophobic interactions; burial of interfacial surface area (31) and/or the presence of waters buried in the interface (32–35) have been suggested to be contributors. While the large changes in ΔCp produced by relatively conservative mutations in this study argue against the former (Table II), water uptake values estimated using the method of Spolar and Record (36) argue in favor of the latter. The number of water molecules taken up by each mutant complex was estimated to be less from that of the wild-type interaction (wt Fab/HEL, 17; $E50_HD$/HEL, 16; $E50_HQ$/HEL, 10; wt Fab/BQL, 10; $E50_HD$/BQL, 4). Along with the large changes in affinity and enthalpy seen in the mutant interactions, this result is consistent with a less well ordered interface, leading to a lower water capture contribution to ΔCp. Structural analysis of mutant complexes now underway may address these issues.

Changes in the Specificity of the Interaction—Each mutation reduces the specificity of the interactions, increasing cross-reactivity. The $E50_HD$ mutation decreased the affinity of HyHEL-5 interaction with HEL by 400-fold; with BQL, less than 10-fold. The $E50_HQ$ mutation decreased the affinity of the interaction with HEL by 40,000-fold; with BQL, 55-fold. Each mutation reduces the affinity of the Fab for HEL much more than for BQL, reducing the specificity and increasing the cross-reactivity of the interaction by 61- or 727-fold, respectively.

These data point to the importance of the electrostatic interactions and the shape complementarity seen in the association of HyHEL-5 Fab with HEL. The side chains of the amino acid mutations in the Fab may pack differently leading to new bonding patterns or to the introduction of water molecules into newly formed cavities in the interface. Structural analysis may assist in understanding these data; very subtle structural changes in other complexes have been shown to produce affinity changes from 10-fold (37) to 1000-fold (8).

Thermodynamic Cycle Analysis of Mutant Interactions—Double-mutant cycles were constructed to test the expectation that the $E50_H$ mutations and the R68K substitution in BQL perturb the same critical interactions (Table III; Fig. 3). In each of the interactions examined, the sum of the $\Delta\Delta G°$ of the single mutations differed from $\Delta\Delta G°$ for the double mutation. The effect of each double mutation is well less than the sum of the effects of individual mutations, confirming that the same interactions are perturbed (26). The calculated coupling energies in these interactions are comparable to the 3.5 to 4.3 kcal mol^{-1} attributed to buried salt links in the folding pathway of barnase (38) and in an anti-HIV Fv/peptide interaction (25).

Conclusion—By mutating a single residue in the HyHEL-5 Fab involved in a buried salt bridge, the affinity of the interaction with HEL was decreased up to 100,000-fold, corresponding to a decrease in $\Delta G°$ of over 8 kcal mol^{-1}. Our results verify the predicted importance of $E50_H$ in the interaction; we find this to be a "hot spot" in the functional epitope. The energy changes can be assigned almost entirely to enthalpic contributions and are among the highest reported $\Delta\Delta H°$s for a single mutation. This result is in contrast to those reported for the deletion of salt bridges in a more heavily solvated environment in the interface between another anti-lysozyme antibody, HyHEL-10, and HEL (28). The mutations studied in this work also greatly reduce the specificity of the antibody for HEL. Crystallographic analyses presently underway should aid in further understanding the overall association process.

REFERENCES

1. Cohen, G. H., Davies, D., and Sheriff, S. (1996) *Acta Cryst. Sect. D* **52,** 315–326
2. Grivel, J. C., and Smith-Gill, S. J. (1996) *Structures of Antigens* **3,** 92–144
3. Padlan, E. A. (1994) *Mol. Immunol.* **31,** 169–217
4. Smith-Gill, S. J., Lavoie, T. B., and Mainhart, C. R. (1984) *J. Immunol.* **133,** 384–393
5. Smith-Gill, S. J., Mainhart, C. R., Lavoie, T. B., Rudikoff, S., and Potter, M. (1984) *J. Immunol.* **132,** 963–967
6. Sheriff, S., Silverton, E. W., Padlan, E. A., Cohen, G. H., Smith-Gill, S. J., Finzel, B. C., and Davies, D. R. (1987) *Proc. Natl. Acad. Sci. U. S. A.* **84,** 8075–8079
7. Chacko, S., Silverton, E., Kam-Morgan, L., Smith-Gill, S., Cohen, G., and Davies, D. (1995) *J. Mol. Biol.* **245,** 261–274
8. Chacko, S., Silverton, E. W., Smith-Gill, S. J., Davies, D. R., Shick, K. A., Xavier, K. A., Willson, R. C., Jeffrey, P. D., Chang, C. Y., and Sheriff, S. (1995) *Proteins Struct. Funct. Genet.* **26,** 55–65
9. Shick, K. A., Xavier, K. A., Rajpal, A., Smith-Gill, S. J., and Willson, R. C. (1997) *Biochim. Biophys. Acta* **1340,** 205–214
10. Hibbits, K. A., Gill, D. S., and Willson, R. C. (1994) *Biochemistry* **33,** 3584–3590
11. Xavier, K. A., Smith-Gill, S. J., and Willson, R. C. (1998) *Biophys J.* **74,** 1–10
12. Novotny, J., Bruccoleri, R. E., and Saul, F. A. (1989) *Biochemistry* **28,** 4735–4749
13. Kozack, R. E., and Subramaniam, S. (1993) *Protein Sci.* **2,** 915–926
14. Slagle, S. P., Kozack, R. E., and Subramaniam, S. (1994) *J. Biomol. Struct. Dyn.* **12,** 439–456
15. McDonald, S. M., Willson, R. C., and McCammon, J. A. (1995) *Protein Eng.* **8,** 915–924
16. Wibbenmeyer, J. A., Xavier, K. A., Smith-Gill, S. J., and Willson, R. C. (1999) *Biochim. Biophys. Acta* **1430,** 191–202
17. Kunkel, T. A. (1985) *Proc. Natl. Acad. Sci. U. S. A.* **82,** 488–492
18. Aune, K. C., and Tanford, C. (1969) *Biochemistry* **8,** 4579–4585
19. Wiseman, T., Williston, S., Brandts, J. F., and Lin, L.-N. (1998) *Anal. Biochem.* **179,** 131–137
20. Lewis, M. S., Shrager, R. I., and Kim, S.-J. (1994) in *Modern Analytical Ultracentrifugation* (Schuster, T. M., and Laue, T. M., eds) Birkhäuser, Boston
21. Press, W. H., Teukolsky, S. A., Vetterling, W. T., and Flannery, B. P. (1992) *Numerical Recipes in C. The Art of Scientific Computing*, 2nd Ed., p. 693, (corrected 1994), University Press, Cambridge
22. Bevington, B. R., and Robinson, D. K. (1992) *Data Reduction and Error Analysis for the Physical Sciences,* Mc-Graw-Hill, New York
23. Lavoie, T. B., Drohan, W. N., and Smith-Gill, S. J. (1992) *J. Immunol.* **148,** 503–513
24. Clackson, T., and Wells, J. A. (1995) *Science* **267,** 383–386
25. Faiman, G. A., Levy, R., Anglister, J., and Horovitz, A. (1996) *J. Biol. Chem.* **271,** 13829–13833
26. Goldman, E. R., Dall'Acqua, W., Braden, B. C., and Mariuzza, R. A. (1997) *Biochemistry* **36,** 49–56
27. Ross, P. D., and Subramanian, S. (1981) *Biochemistry* **20,** 3096–3102
28. Tsumoto, K., Nakaoki, Y., Ueda, Y., Ogasahara, K., Yutani, K., Watanabe, K., and Kumagai, I. (1996) *J. Biol. Chem.* **271,** 32612–32616
29. Benjamin, D. C., Williams, D. C., Jr., Smith-Gill, S. J., and Rule, G. S. (1992) *Biochemistry* **31,** 9539–9539
30. Deleted in proof
31. Murphy, K. P., and Freire, E. (1992) *Adv. Protein Chem.* **43,** 313–361
32. Bhat, T. N., Bentley, G. A., Boulot, G., Greene, M. I., Tello, D., Dall'Acqua, W., Souchon, H., Schwarz, F. P., Mariuzza, R. A., and Poljak, R. J. (1994) *Proc. Natl. Acad. Sci. U. S. A.* **91,** 1089–1093
33. Goldbaum, F. A., Schwarz, F. P., Eisenstein, E., Cauerhiff, A., Mariuzza, R. A., and Poljak, R. J. (1996) *J. Mol. Recog.* **9,** 6–12
34. Raman, C. S., Allen, M. J., and Nall, B. T. (1995) *Biochemistry* **34,** 5831–5838
35. Xavier, K. A., Shick, K. A., Smith-Gill, S. J., and Willson, R. C. (1998) *Biophys. J.* **73,** 2116–2125
36. Spolar, R. S., and Record, M. T., Jr. (1994) *Science* **263,** 777–784
37. Tulip, W. R., Harley, V. R., Webster, R. G., and Novotny, J. (1994) *Biochemistry* **33,** 7986–7997
38. Tissot, A. C., Vuilleumier, S., and Fersht, A. R. (1996) *Biochemistry* **35,** 6786–6794

Salt Links Dominate Affinity of Antibody HyHEL-5 for Lysozyme through Enthalpic Contributions

Jamie A. Wibbenmeyer, Peter Schuck, Sandra J. Smith-Gill and Richard C. Willson

J. Biol. Chem. 1999, 274:26838-26842.
doi: 10.1074/jbc.274.38.26838